Electrical activity of chalcogen-hydrogen defects in silicon

J. Coutinho* and V. J. B. Torres
Department of Physics, University of Aveiro, 3810 Aveiro, Portugal

R. Jones
School of Physics, University of Exeter, Stocker Road, Exeter, EX4 4QL, United Kingdom

P. R. Briddon
Department of Physics, University of Newcastle upon Tyne, Newcastle upon Tyne, NE1 7RU, United Kingdom
(Received 5 August 2002; published 24 January 2003)

The interaction of hydrogen with substitutional chalcogen impurities (S, Se, or Te) is investigated by *ab initio* modeling. In Se-H_n and Te-H_n complexes ($n=1,2$), protons are located at sites antibonding to nearest-neighbor silicon atoms. For sulfur, two competitive sites for S-H are found, resulting in two nearly degenerate structures. All the singly hydrogenated complexes are predicted to be shallow donors with levels lying above those of the substitutional S, Se, and Te double donors. In contrast, doubly hydrogenated chalcogen impurities are predicted to be electrically inert. A comparison of our results with experimental data suggests that the NL60 and NL61 electron-paramagnetic-resonance centers can be identified with two Se-H defects, where H is antibonded to a Si neighbor of Se.

DOI: 10.1103/PhysRevB.67.035205 PACS number(s): 61.72.Bb, 61.72.Ji, 61.72.Yx, 85.40.Ry

I. INTRODUCTION

The single and close-by pairs of chalcogen impurities are perhaps the best characterized double-donor defects in silicon.[1] As single impurities, they are known to occupy a T_d symmetric site, whereas chalcogen pairs form a D_{3d} structure. In both cases, they are generally considered to be substitutional defects.[2] All the centers, S_s, Se_s, Te_s, S_{2s}, Se_{2s}, and Te_{2s}, denoted by X_s and X_{2s}, possess deep $(0/+)$ and $(+/++)$ donor states between $\sim$0.2 and $\sim$0.6 eV, respectively, below the conduction-band bottom. They have been investigated using electronic infrared (IR) absorption and deep-level transient spectroscopy (DLTS), as well as electron paramagnetic resonance (EPR).[1,3–7] The calculation of electrical levels of defects is now of major interest, and the chalcogen double donors and their interaction with hydrogen provide a good test for theoretical techniques. The traditional way in which they are found is to estimate the formation energies of charged defects taking into account some correction for the compensating background, which must be present in periodic supercell calculations to ensure a finite energy per cell.[8,9] This method, however, has occasionally given some disappointing results in the past, with the $(-/0)$ level of VO in Si found 0.4 eV above $E_{\rm v}$,[10] rather than the measured 0.17 eV below $E_{\rm c}$.[11,12] We shall describe here a method that appears to provide better results, and in which we compare the ionization energies of defects with those of other defects[13–15] or the bulk crystal.[16] In this way, systematic errors in the treatment of charged cells can be largely eliminated.

The interaction between hydrogen and dopant impurities is a well-known phenomenon with important technological consequences.[17] Hydrogen is also known to remove, create, or displace defect-related levels, and a detailed characterization of this interaction is highly desirable. Here we deal with both partial and complete passivation of substitutional chalcogen double donors.

Chalcogen-hydrogen complexes have been studied by several experimental techniques, including electron paramagnetic resonance, electron-nuclear double resonance (ENDOR),[18,19] Fourier-transform infrared (FTIR) spectroscopy,[20] DLTS,[21,22] and time-dependent conversion electron Mössbauer spectroscopy (CEMS).[23] The S-H defects were prepared by diffusing sulfur and hydrogen into n-Si at high temperatures followed by a rapid quench.[18] From EPR and ENDOR experiments, sulfur is known to trap hydrogen and form two distinct trigonal S-H defects labeled as NL54 and NL55. Their g values are very similar, and a clear resolution is only attained when the more sensitive ENDOR measurements were used. Isotopic enrichment studies showed that each contained one S atom. Interactions with a single H atom on each center were also observed in ENDOR. Analysis of the ^{33}S and ^{1}H hyperfine interactions showed the spin densities on S and H to be 5.89% and 0.33% in NL54, and 5.54% and 0.39% in NL55, respectively. In similarly prepared samples, FTIR measurements revealed four effective-mass absorption series with binding energies lying between 82.4 and 135.45 meV, possessing clear deuterium isotopic shifts.[18,20] These experiments strongly suggest that both S-H defects are shallow effective-mass-like donors that are observed in their neutral charge states. DLTS measurements on hydrogenated chalcogen-doped Si crystals revealed a loss of the chalcogen-related levels, caused either by complete hydrogen passivation, or the introduction of levels too shallow to be detected by this technique.[21]

Early semiempirical calculations suggested that full passivation of S_s could occur with a *single* hydrogen atom.[24] However, later work found two almost degenerate S-H structures that could behave as single donors.[25]

Selenium is also known to complex with hydrogen. In the

 ©2003 The American Physical Society

EPR and ENDOR experiments, selenium and hydrogen were introduced into p-Si by thermal diffusion around 1350 °C and the samples rapidly quenched.[19] Two trigonal EPR centers NL60 and NL61 were found. The first one contains a single Se and H atom, but NL61, with a very similar g tensor, has been assigned to either $(\text{Se-H}_2)^{+/-}$ or to two distinct Se-H complexes with nearly identical g values.[19] As far as we know, no attempt to model these complexes has been reported.

Tellurium-hydrogen complexes have been studied by CEMS, where the decay of ^{119}Te-H and ^{119}Te-H_2 complexes to the well studied ^{119}Sb-H and ^{119}Sb-H_2 defects provided evidence that H occupies the same site in all defects, i.e., antibonded to the Si atoms neighboring Te or Sb atoms.[23] This structure was recently reproduced by *ab initio* pseudopotential calculations, but its electrical activity has not been investigated.[26] Previous modeling also suggested that the reaction of S-H with a second H atom is exothermic, ending with an electrically inert S-H_2 complex.[24]

In this paper we study S-H_n, Se-H_n, and Te-H_n complexes, with special attention to their electronic and vibrational properties, and we compare these with O-H_n defects. In Secs. II and III, we describe the method and discuss the convergence of the properties of the defects, especially the ionization energies, with basis sets, etc. Then, in Secs. IV–VI, we give our results on X_{ns} and X-H_n defects. Our conclusions are given in Sec. VII.

II. METHOD

We employ a spin-polarized, local-density-functional supercell code AIMPRO,[27,28] together with a Perdew-Wang exchange-correlation energy parametrization.[29] Bachelet-Hamann-Schlüter pseudopotentials are used and eliminate the need to include core electrons.[30] The X_s, X_{2s}, X-H, and X-H_2 complexes are introduced in otherwise perfect 64 (cubic), 96 (orthorhombic), and 216 (cubic) Si-atom cells. The energies of these cells were found and the structures relaxed at fixed volume. All these calculations used eight special **k** points generated by a Monkhorst-Pack scheme (MP-2^3).[31] Calculations of the Mulliken populations describing the localization of the spin density were carried out in 216-Si-atom supercells, containing structures found from the 64-Si-atom cell, and again the MP-2^3 special **k** points were used.

The wave functions are expanded in N real space s,p Cartesian-Gaussian orbitals centered on each atom, and M at the center of bonds. For S, Se, Te, we used $(N,M)=(5,1)$. For O, H, and Si, $(N,M)=(6,1)$, (2,1), and (4,1) respectively.[28] The bond-center orbitals are important in order to reproduce high angular momentum hybridizations. The energy cutoff E_{cut} for the Fourier expansion of the charge density was 50 Ry, except when O was present where $E_{\text{cut}}=150$ Ry. Higher cutoffs led to energy changes of less than $\sim$1 meV. Further details about the method can be found elsewhere.[28]

Of special interest to this study are the ground-state structure, local vibrational mode (LVM) frequencies, and the electrical levels. LVM frequencies were obtained from the second derivatives of the total energy with respect to the positions of the defective atoms and their Si neighbors. The contributions to the dynamical matrix from other Si atoms in the supercell were found from a Musgrave-Pople interatomic potential given earlier.[27,32]

There is no accepted procedure for calculating the energy levels of defects. One way is to evaluate their formation energies in different charge states. We refer to this as the *formation energy method* (FEM), and is discussed in Ref. 33. Here, the formation energy E_{f} of a charged defect with an excess of positive charge q is given by

$$E_{\text{f}}(q)=E_{\text{d}}(q)-\sum_i n_i\mu_i+q(E_{\text{v}}+\mu_{\text{e}})+\alpha_{\text{M}}\frac{q^2}{L\epsilon}, \quad (1)$$

where $E_{\text{d}}(q)$ is the energy of the defective supercell, made up of n_i atom species with chemical potential μ_i, and μ_{e} is the Fermi energy of the electrons relative to the valence-band top E_{v}. The valence-band top in the defective cell is shifted from its value in the bulk by a potential term. This, together with the other terms, is evaluated by following the procedure given in the Appendix. The last term in Eq. (1) is the usual monopole correction, that subtracts the energy of an array of charges q embedded in a compensating uniform charge density.[34] Here α_{M} is the Madelung constant, L is a lattice parameter, and ϵ the permittivity of the material.

The formation energy controls the equilibrium concentration of defects in the material. The chemical potentials are related to the energy per atom on its *standard* phase. Their values for Si and H species are found from their energies in the crystalline and molecular forms, respectively. For the chalcogen species, we also used their standard phases, i.e., the spin-1 O_2 molecule, solid monoclinic α-S and α-Se, and trigonal Te, respectively.

Another method that has been used to estimate energy levels compares the ionization energies of defects, or more strictly $E_{\text{d}}(q+1)-E_{\text{d}}(q)$, with standard defects whose electrical levels are known.[13–15] This method works best when the defect under consideration and the marker have close-by levels. For a particular defect marker D, we will denote the method by MM(D). We notice that terms like the Madelung correction shift both the marker and the defect by the same amount, and hence systematic errors are largely eliminated. Alternatively, it has been suggested that these ionization energies can be compared with the same expression evaluated for bulk material in a similarly sized cell.[16] In this case, the energies of bulk supercells when a hole is added to the top of the valence band, or an electron to the bottom of the conduction band, are required. This method is denoted by MM(Si). The donor level is referred to the conduction band by adding the experimental band-gap energy (1.17 eV). Some care needs to be taken in calculating the energies of charged host and defective cells as the occupied bands can have wide dispersion. Accordingly, states in the valence and conduction bands are occupied as for a metal. Nevertheless, we find that this method seriously underestimates the correlation energy and the best method is when the ionization energies are compared with other defects as in the MM(D) technique.

Hyperfine and super-hyperfine interactions measured by EPR/ENDOR are often analyzed by expressing the spin den-

TABLE I. Convergence tests for total energies of neutral and positive charge states, ionization energy I, and donor level $[E_c - E(0/+)]$ for the H_2S molecule and substitutional sulfur in silicon (Si:S_s), respectively. Chemical potentials of S (in α-sulfur) and Si (in bulk Si), as well as the formation energy E_f of Si:S_s, are also included. All values are in eV. *Standard* calculations are carried out with one set of bond-center functions, MP-2^3 for Brillouin-Zone BZ sampling, 50-Ry plane-wave cut-off, and a 64-Si-atom supercell. Test calculations consist in using two sets of bond-center functions (2BC) with $E_{cut}=75$ and 100 Ry. The energy E_{mol} for H_2S^+ includes a Madelung correction of 1.2867 eV.

	H_2S			Si:S_s					
Test	$E_{mol}(0)$	$E_{mol}(+)$	I	$E(0)$	$E(+)$	$E_c - E(0/+)$	μ_S	μ_{Si}	E_f
Standard	−309.0786	−298.5663	10.5123	−7072.1716	−7079.1723	0.4333	−278.3088	−107.8552	1.0148
2BC	−309.4475	−298.9401	10.5074	−7075.6112	−7082.5433	0.4375	−278.4489	−107.9073	0.9976
$E_{cut}=75$	−309.0790	−298.5666	10.5124	−7072.1717	−7079.1946	0.4110	−278.3088	−107.8552	1.0147
$E_{cut}=100$	−309.0788	−298.5664	10.5124	−7072.1717	−7079.1946	0.4110	−278.3088	−107.8552	1.0147
Observed			10.453 [a]			0.29 [b]			

[a]Reference 35.
[b]Reference 36.

sity in terms of an orbital written as a linear combination of s and p atomic orbitals (LCAO).[12] Thus the defect state is characterized in terms of the percentage of s- or p-orbital character. Here we relate these quantities to the Mulliken bond population of the highest occupied spin level. These populations are found in 216-atom cells, by averaging over the Brillouin zone of the highest occupied band.[14]

III. CONVERGENCE TESTS

A number of convergence issues are involved in our calculations, e.g., the sizes of the real basis set used to expand the wave functions, and the reciprocal-space basis used to fit the charge density. In addition, the supercell size and number of special **k** points are important quantities that can affect the results.

The effect of a different basis on the energies of a H_2S molecule and the substitutional sulfur defect in a 64-atom cell of Si are shown in Table I. The total energy E_{mol} of a single charged molecule in a periodic calculation, taking into account the Madelung term, is

$$E_{mol}(q) = E(q) + \alpha_M \frac{q^2}{L}, \tag{2}$$

where $E(q)$ is the energy per cell with a charged molecule. The ionization energy of the molecule is given by $I = E_{mol}(q+1) - E_{mol}(q)$. The length of the cell was increased up to $L=40$ Å until the energy change became negligible (<5 meV, see Fig. 1). The dependence of the energy on L comes from the interaction of molecular dipoles in different cells although there is a counterdipole introduced by a jellium in each cell. Nevertheless, there is a dependence on the energy coming from the stacking of the molecular dipoles, which can be estimated by placing a pair of inverted molecules within each cell. If the cell energies are E_{H_2S} and E_{2H_2S}, respectively, then Fig. 1 shows the variation of $\Delta E_{dpol} = E_{2H_2S}/2 - E_{H_2S}$ with L and demonstrates that the different stackings of dipoles only changes the energy per molecule by about 5 meV.

For this molecular problem, different **k**-point sampling meshes, e.g., Γ, MP-2^3, and MP-4^3 gave identical energies, demonstrating the lack of dispersion in the band structure (i.e., the electronic interaction between the molecules in different cells). Table I gives the energies of H_2S and of substitutional sulfur defect in silicon found for different basis sets and cutoffs. It is clear that total energies are converged when $E_{cut}>50$ Ry is used. The effect, however, of augmenting the *standard* basis with an additional set of s- and p-orbital sites at each bond center is large for the total energy but has little effect, less than 0.1 eV, on the ionization energy of H_2S and the formation energy of sulfur in Si evaluated in a 64-atom cell. We note that there the calculated ionization energy of H_2S is improved by ~1.3 eV through the inclusion of the Madelung energy correction. It is also clear here that, despite

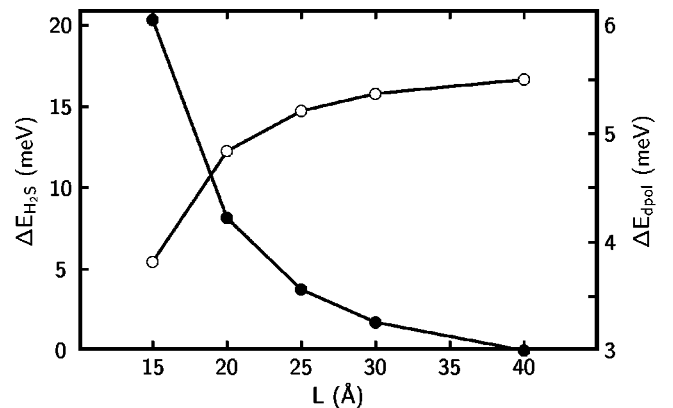

FIG. 1. Relative energy of a H_2S molecule (ΔE_{H_2S}) in several sized supercells (filled circles), and electric dipole correction energy (ΔE_{dpol}) in opened circles. The dipole term was obtained by comparing energies of a supercell containing one H_2S molecule with that of a cell, twice the size along the dipole direction, and containing a second inverted molecule.

TABLE II. Calculated donor levels [(0/+) and (+/++)] for S_s in Si. Marker and formation energy methods were used with 64- and 216-Si-atom supercells. All values are given in eV. The influence of charge and asymptotic potential corrections are also considered. First and second ionization energies are to be compared with measurements of $E_c-0.29$ and $E_c-0.59$ eV respectively (Ref. 1). Asymptotic potentials $\bar{V}$ and Coulomb correction (see text) are also included.

	64 Si			216 Si		
		$E_c-(0/+)$	$E_c-(+/++)$		$E_c-(0/+)$	$E_c-(+/++)$
MM(Si)		0.4333	0.4677		0.6127	0.6169
FEM		0.7774	1.2538		0.6798	1.1185
FEM [a]		0.6195	0.7800		0.5745	0.8026
FEM [b]		0.7062	1.0718		0.6473	0.9998
q	0	+	++	0	+	++
E_d	−7072.1716	−7079.1723	−7086.1233	−23466.3523	−23473.3594	−23480.2246
E_{bulk}	−6902.7299	−6908.9939	−6915.2426	−23296.9848	−23303.4346	−23309.7467
ϵ^0_{bulk}	6.3790			6.3791		
$\bar{V}_{bulk}$	9.7847			9.7870		
$\bar{V}_d$		9.8559	9.9113		9.8195	9.8626
$\alpha_M(2q+1)/L\epsilon$		0.1579	0.4738		0.1053	0.3159

[a]Without Madelung correction.
[b]Without potential correction.

the variation in the absolute energy with basis, convergence has been obtained for all other parameters. The calculated ionization energies for H_2S were compared with the experimental values of 10.453 eV.[35]

We now turn to the sulfur defect in Si. The convergence of the total energies $E(0)$ and $E(+)$ is shown in Table I. Although these energies, along with the chemical potential, vary appreciably with basis, the formation energy E_f, being about 1 eV, does not. We now consider the calculation of electrical levels. The formation energy method as described in the Appendix leads to the (0/+) level of S between $E_c-0.57$ eV and $E_c-0.77$ eV depending on the inclusion of Madelung and potential corrections. The (+/++) levels lie between $E_c-0.78$ eV and $E_c-1.2$ eV (Table II). These values are relatively insensitive to **k**-point sampling and to the size of the unit cell. The (0/+) and especially the (+/++) levels are far too deep when compared with experimental values of $E_c-0.29$ and $E_c-0.59$ eV.[36]

The MM(Si) method, described in more detail in the Appendix, leads to (0/+) and (+/++) levels around 0.4 and 0.5 eV in the 64-atom cell, and about 0.2 eV deeper in the 216-atom cell, respectively (Table II). These shift 0.5 and 0.4 eV for MP-6^3 sampling in the 64-atom cell (Table III). Thus the latter predicts a negative-U ordering of the levels in conflict with experiment. Clearly, the correlation energy is not at all treated accurately. Despite this disappointing result for the levels, we shall show below that much better results arise if we compare the calculated levels of a defect with those of sulfur. In this way systematic errors appear to be eliminated.

Table IV shows how structural parameters, vibrational frequencies, and ionization energies of the well known H_2O, H_2S, H_2Se, and H_2Te molecules compare with experiment. We find excellent agreement, to within ~2% for structures, ~8% for LVM's, and about 0.2 eV for energetics (enthalpy of formation and ionization energies).

In summary, we have checked the sensitivity of the total energies and structures with basis, energy cutoff, **k**-point sampling, and unit-cell size. Only structures and differences in energy are converged, but electrical levels (as calculated by the formation or ionization energy methods), are too deep.

IV. SUBSTITUTIONAL CHALCOGEN DEFECTS

Previous theoretical modeling found, in agreement with experiment, that S, Se, and Te favor substitutional sites in Si.[2] Our calculations support this as the formation energies of neutral S, Se, and Te at interstitial T sites are 3.0, 3.8, and 5.5 eV, respectively, less favorable than the substitutional impurities. In contrast with substitutional oxygen,[28] the single-chalcogen defects show no tendency to move off their lattice site. The formation energy of a substitutional sulfur impurity controls its solubility. Sulfur doping is commonly attained by in diffusion into Si at ~1200 °C in a mixed atmosphere of sulfur and He.[20,22,38] Using this procedure, concentrations of S_s and S_{2s} are normally of the order of 10^{15}–10^{16} cm^{-3}, suggesting a formation energy of around 1.7 eV, considerably greater than 1 eV found here for S_s. The discrepancy with experiment with regard to the solubility of sulfur might be related to the difficulty of estimating its chemical potential, or that there is a substantial energy barrier at the surface preventing its incorporation.

Pairing of X impurities is highly favorable for S and Se, showing binding energies above 1 eV. Table V gives the formation energies per X atom for the chalcogen pairs. Bind-

TABLE III. Quantities used to evaluate energy levels of S_s using several special **k**-point sets. These include total energies of bulk and defective cell (E_{bulk} and E_d), highest occupied state in bulk (ϵ^0_{bulk}), and asymptotic potentials $\bar{V}$. All calculations use 64-Si-atom supercell, 50 Ry energy cutoff, and (4,1) and (5,1) basis sets for Si and S species, respectively. Madelung correction is made with $\alpha_M = 1.4186$, $L = 20.370$ a.u., and $\epsilon = 12$. All energies are given in eV. First and second ionization energies are to be compared with measurements of $E_c - 0.29$ and $E_c - 0.59$ eV, respectively (Ref. 1).

Sampling	MP-2^3	MP-4^3	MP-6^3
$E_{bulk}(0)$	−6902.7299	−6902.8125	−6902.8126
$E_{bulk}(+)$	−6908.9939	−6909.2136	−6909.2008
$E_{bulk}(++)$	−6915.2426	−6915.3999	−6915.4012
ϵ^0_{bulk}	6.3790	6.3781	6.3781
$\bar{V}_{bulk}$	9.7847	9.7870	9.7870
$E_{bulk}(0) - E_{bulk}(+)$	6.2640	6.4011	6.3882
$E_{bulk}(+) - E_{bulk}(++)$	6.2487	6.1863	6.2004
$E_d(0)$	−7072.1716	−7072.1701	−7072.1658
$E_d(+)$	−7079.1723	−7079.2353	−7079.2179
$E_d(++)$	−7086.1233	−7086.2101	−7086.2105
$\bar{V}_d(+)$	9.8559	9.8593	9.8594
$\bar{V}_d(++)$	9.9113	9.9139	9.9132
$E_d(0) - E_d(+)$	7.0007	7.0652	7.0521
$E_d(+) - E_d(++)$	6.9510	6.9748	6.9926
$\mathcal{E}_v(0/+)$	6.6081	6.6083	6.6084
$\mathcal{E}_v(+/++)$	7.0348	7.0334	7.0319
$E_c - (0/+)$ MM(Si)	0.4333	0.5059	0.5061
$E_c - (+/++)$ MM(Si)	0.4677	0.3815	0.3778
$E_c - (0/+)$ FEM	0.7774	0.7131	0.7263
$E_c - (+/++)$ FEM	1.2538	1.2285	1.2093

ing energies above 1 eV are also predicted for mixed pairs (S-Se, S-Te, and Se-Te). The Te_{2s} complex is less likely to form, perhaps explaining the poorer knowledge regarding this complex.

Structural details of X_s and X_{2s} defects from Table V show that X-Si and X-X bond lengths increase monotonically with the impurity size. The one-electron band structures of all the substitutional chalcogen defects and related pairs possess a fully occupied singlet state at the middle of the band gap. This is shown in Fig. 2 for the case of S_s and S_{2s} defects. The donor levels of these defects were found as discussed above and are given in Table V.

Using the MM(Si) method, the first donor level of each defect is *systematically* too deep by ~0.1 eV while the sec-

TABLE IV. Comparison between calculated and measured properties of H_2X molecules. Experimental data (Ref. 37) include enthalpy of formation of the gas phase, $\Delta_f H^0(g)$ [at 0 °C and 1 bar, from standard phases of H and O (molecular), and S, Se, and Te (solid)], X-H bond length, H-X-H angle, ionization energy I, electron affinity A, asymmetric and symmetric stretch mode frequencies ν^s_{B1} and ν^s_{A1}, and bend mode ν^b_{A1}. Bond lengths, angles, energies, and frequencies are given in angstrom, degrees, eV, and cm^{-1} respectively.

	H_2O		H_2S		H_2Se		H_2Te	
Observable	Calc.	Expt.	Calc.	Expt.	Calc.	Expt.	Calc.	Expt.
$\Delta_f H^0(g)$	−2.77	−2.51	−0.42	−0.21	0.36	0.31	0.82	1.03
X-H	0.981	0.957	1.371	1.335	1.478	1.461	1.664	1.691
Angle	105.8	104.5	91.5	92.1	90.2	90.2	89.7	89.5
I	12.76	12.65	10.51	10.45	9.87	9.89	9.09	9.14
A	3.58	3.61						
ν^s_{B1}	3757	3756	2634	2626	2402	2358	2134	NA
ν^s_{A1}	3651	3657	2618	2615	2380	2345	2130	NA
ν^b_{A1}	1480	1595	1088	1183	983	1034	834	NA

TABLE V. Calculated (Calc.) formation energies E_{f}, binding energies E_b, bond lengths, electrical levels, experimental levels (Expt.) in eV (Ref. 1), and spin localization for substitutional chalcogen impurities in silicon. Levels calculated using the marker [MM(Si) and MM(S)] and formation energy methods (with Madelung and potential corrections) are given. Spin localization on the X atom (η_X^2) and on its four Si nearest neighbors (η_{nn}^2) obtained from the Mulliken bond populations are given in percent. The p character (β_{nn}^2) of the donor wave function on these Si ligands (%) is also shown and compared with the LCAO analysis from respective EPR signals (Refs. 5,38–40). NA stands for not available.

						$E_{\mathrm{c}}-E(+/0)$			$E_{\mathrm{c}}-E(++/+)$					
		E_{f}	E_b	X-Si	X-X	MM(Si)	MM(S)	FEM	MM(Si)	MM(S)	FEM	η_X^2	η_{nn}^2	β_{nn}^2
S_s	Calc.	1.01		2.444		0.43	0.29	0.78	0.48	0.59	1.25	6.6	48	97
	Expt.						0.29			0.59		9	52	$\sim$91
S_{2s}	Calc.	0.34	1.68	2.295	3.088	0.25	0.13	0.59	0.25	0.35	1.04	2.8	5	95
	Expt.						0.19			0.39		4.1	NA	NA
Se_s	Calc.	1.48		2.520		0.40	0.28	0.79	0.45	0.55	1.32	6.6	43	98
	Expt.						0.29			0.54		10	NA	NA
Se_{2s}	Calc.	1.80	1.16	2.390	3.090	0.27	0.15	0.69	0.26	0.36	1.13	2.7	4	95
	Expt.						0.21			0.39		4.2	NA	NA
Te_s	Calc.	1.97		2.635		0.27	0.15	0.75	0.28	0.38	1.22	6.4	38	100
	Expt.						0.20			0.36		11	40	96
Te_{2s}	Calc.	3.42	0.52	2.531	3.213	0.20	0.08	0.80	0.20	0.30	1.25	3.3	4	99
	Expt.						0.16			NA		NA	NA	NA
S_s-Se_s	Calc.	1.04	1.45	2.292;2.392	3.063	0.23	0.11	0.61	0.26	0.36	1.10	2.1;3.6	6;5	96;90
	Expt.						NA			NA		NA	NA	NA
S_s-Te_s	Calc.	1.64	1.34	2.307;2.547	3.128	0.17	0.05	0.61	0.21	0.31	1.10	1.2;5.5	7;2	99;93
	Expt.						NA			NA		NA	NA	NA
Se_s-Te_s	Calc.	2.42	1.03	2.419;2.546	3.169	0.16	0.04	0.65	0.19	0.29	1.13	1.9;5.3	8;1	100;89
	Expt.						NA			NA		NA	NA	NA

ond donor level is too shallow by about 0.1 eV. This demonstrates that much better prediction of the levels of say Se and Te can be achieved by comparing their ionization energies with those of sulfur [MM(S) method]. This places the Se levels at the same position as S, and the Te $(0/+)$ and $(+/++)$ levels 0.15 eV and 0.1 eV, respectively, above those of S, in very good agreement with experiment. The same is true for defect pairs. The calculated levels are $\sim$0.05 eV different from those observed. The effect of a wide dispersion in the defect-related bands appear to cancel in the MM(S) method probably because the defects have the same symmetry and the wave functions are of the same extent. Levels found from the formation energy method are too deep. In fact, X_{s} defects are predicted to be single donors. Despite this, the results provide a reference for comparison with levels from X-H defects. It is also noteworthy that the relative level positions of the three chalcogen impurities are well reproduced, with the S and Se levels lying close together, well below those of tellurium.

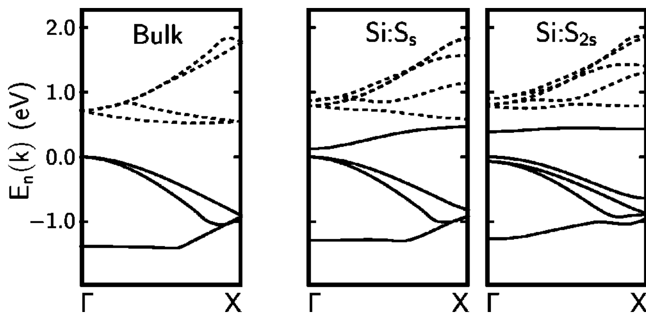

FIG. 2. One-electron band structure for bulk Si, substitutional sulfur (Si:S_{s}), and substitutional sulfur pair defects (Si:$S_{2\mathrm{s}}$). These are evaluated in a 64-Si-atom supercell. Here $X=\pi(100)/2a_0$, where $a_0=5.390$ Å is the calculated bulk lattice parameter. Solid and dotted lines represent occupied and empty levels, respectively. Levels from defective cells were aligned with help of the average potential shift discussed in the Appendix.

Analysis of the Mulliken bond populations for S_{s} in a 64-Si-atom cell gave a localization of $\eta_S^2=7.0\%$ on the sulfur atom, and 45% on the first neighboring ligands. These are to be compared with the volumes of 9% and 52% from ENDOR experiments.[3] The populations were found in larger 216-Si-atom supercells and given in Table V. About $\sim$6% of the spin density is found on the chalcogen impurity, in a fully symmetric s orbital, and about 38–48 % on p orbitals centered at their Si nearest neighbors. These are in good agreement with the $\sim$10% and 52–38 % derived from the analysis of the hyperfine interactions.[5,39] Also in good agreement with the observations are the Mulliken populations for chalcogen pairs. Here we predict the localization on each X atom to be about half of that in X_{s} impurities. We are unaware of any reports on ^{29}Si hyperfine spectra for the chalcogen pairs.

V. INTERACTION WITH ONE HYDROGEN ATOM

There are a number of possible locations for H near the chalcogen impurity, which were investigated. In each case,

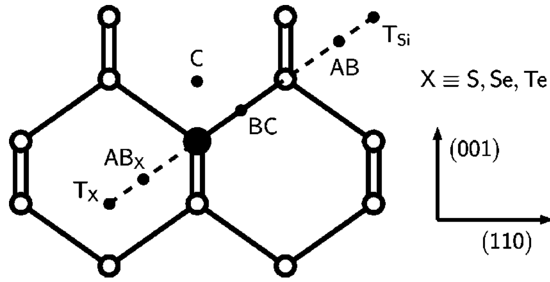

FIG. 3. Some high-symmetry interstitial sites (small black circles) near to a substitutional chalcogen atom (large black circle). Si atoms are white. T, BC, and AB stand for tetrahedral, bond-center, and anti-bonded sites, and the C site lies between second nearest-neighboring Si atoms.

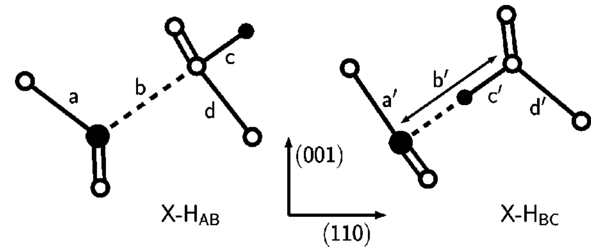

FIG. 4. Low-energy structures for X-H complexes in silicon. These are antibonding to a Si neighbor of X, and are bond centered (X-H_{AB} and X-H_{BC}, respectively). Si, X, and H atoms are shown as open, large-closed, and small-closed circles, respectively. Bond lengths and distances (labeled by $a, \ldots, d$ and $a', \ldots, d'$) are reported in Table VI.

the relaxation of the defects was carried out both with and without a symmetry constraint. Some of the possible sites are shown in Fig. 3 and labeled according to the usual notation. Two tetrahedral (T_X and T_{Si}), two antibonding (AB_X and AB), one bond-centered (BC), and orthorhombic (C) sites were considered.

Interstitial hydrogen in Si is an amphoteric impurity with a negative-U ordering of the $(-/0)$ and $(0/+)$ levels. H^- is expected to be located at a tetrahedral interstitial T site, whereas H^+ is located at a BC site.[41] This suggests that H located at a T or AB site could compensate a nearby chalcogen.[17]

Among all the chalcogen-hydrogen complexes, only two competitive energetic structures were found, namely, the generally stable X-H_{AB} and a metastable X-H_{BC} form (see Fig. 4). As shown in Table VI, their relative energies differ by 0.1, 0.3, and 0.8 eV for S, Se, and Te, respectively. Both these structures possess trigonal symmetry. If the H and X atoms were perturbed, and this symmetry was lost; then on relaxation, both atoms returned to reform the trigonal defect. The energies of metastable centers where H is antibonded to the chalcogen atom (AB_X) are about 1.0 eV higher than the ground state, and therefore unlikely to occur.

The binding energy E_b of H with the chalcogen X_s was also found and is given in Table VI. These were obtained by evaluating the energies of neutral bond-centered H and sub-

TABLE VI. Calculated energies relative to the most stable configuration, E_{rel} (eV), X-H binding energies E_b (eV), donor level $E(0/+)$ (eV), structural parameters (in angstrom, see also Fig. 4), localization η^2 of the donor state on X and H atoms (%), and respective s and p characters α^2 and β^2 (%). Local vibrational mode frequencies ν (cm^{-1}) are labeled according to its representation within the C_{3v} point group and mode type (s for a Si-H stretch mode, and b for a Si-H bend mode).

X	S		Se		Te	
Complex	AB	BC	AB	BC	AB	BC
E_{rel}	0.00	0.13	0.00	0.34	0.00	0.77
E_b	1.66	1.53	1.60	1.25	1.71	0.94
$E_c-E(+/0)$ MM(Si)	0.13	0.26	0.10	0.26	0.00	0.20
$E_c-E(+/0)$ MM(S)	0.01	0.14	−0.02	0.14	−0.12	0.08
$E_c-E(+/0)$ FEM	0.41	0.53	0.37	0.53	0.27	0.47
$E_c-E(++/+)$ MM(Si)	1.18	1.18	1.18	1.19	1.18	1.16
$E_c-E(++/+)$ MM(S)	1.28	1.28	1.28	1.29	1.28	1.26
$E_c-E(++/+)$ FEM	1.78	1.78	1.77	1.78	1.77	1.76
a, a'	2.337	2.315	2.437	2.412	2.578	2.553
b, b'	3.106	3.498	3.025	3.562	2.992	3.625
c, c'	1.551	1.496	1.554	1.499	1.549	1.502
d, d'	2.305	2.301	2.305	2.301	2.304	2.297
η_X^2	5.2	5.0	5.8	5.3	4.5	5.4
α_X^2	55	83	43	75	33	61
β_X^2	45	17	57	25	67	39
η_H^2	0.5	0.3	0.7	0.6	0.3	0.0
α_H^2	82	18	79	13	88	0
β_H^2	18	82	21	87	12	100
$\nu_{A_1}^s$	1857	2141	1842	2127	1842	2110
ν_E^b	772	582	772	567	775	557

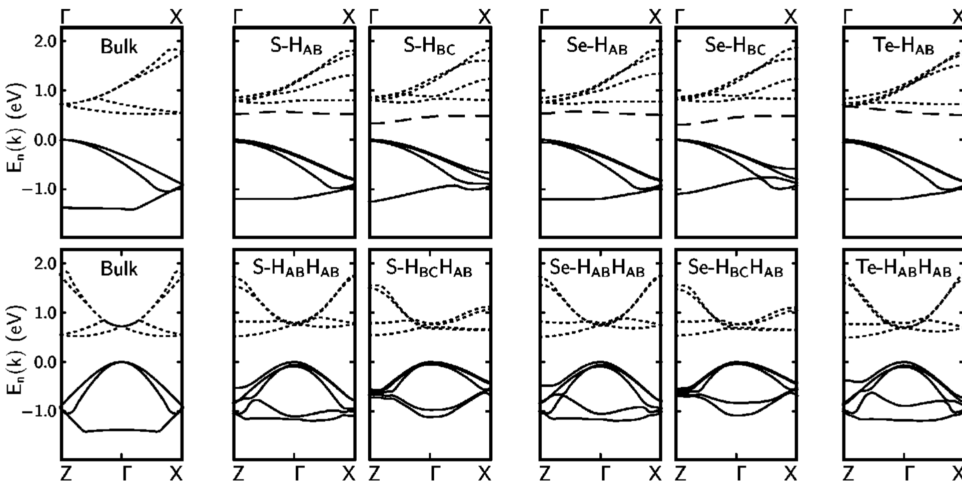

FIG. 5. One-electron band structure for bulk Si, X-H, and X-H_2 defects evaluated in a 64-Si-atom supercell. Here $X = \pi(100)/2a_0$ and $Z = \pi(001)/2a_0$, where $a_0 = 5.390$ is the calculated bulk lattice parameter. Solid, dashed, and dotted lines represent occupied, semioccupied, and empty levels, respectively. Levels from defective cells were aligned with the help of the average potential shift discussed in the Appendix.

stitutional chalcogen atoms in different cells. The difference in energy, ~ 0.2 eV, of the donor and acceptor levels of the chalcogen and hydrogen should be added to this if the constituents are charged. The barrier to the dissociation should be supplemented by the migration energy of H, which probably adds another 0.2 eV. Thus we anticipate a dissociation barrier of around 1.8–2 eV, and is somewhat larger than the observed dissociation barrier lying between 1.39 and 1.61 eV.[22] From the energetics, and in agreement with the time-dependent Mössbauer measurements, we can rule out the Te-H_{BC} structure. For S, the BC and AB structures are degenerate to within the error of the calculations.

Structural details of X-H complexes are shown in Table VI and Fig. 4. For AB defects, the *smaller* the chalcogen atom, the larger its displacement along the trigonal axis. This contrasts with the BC structures where the presence of a strong Si-H bond results in a large distortion b', and therefore higher energies.

The electrical activity of X-H complexes can be appreciated by inspection of the one-electron band structure. These are shown on the top half of Fig. 5, where they are compared with the band structure from a bulk supercell. The half-filled band (dashed line) at the top half of the gap strongly suggests donor activity. The calculated donor levels of X-H defects are given in Table VI.

All the X-H complexes possess donor levels high in the band gap and above the donor levels of the isolated chalcogen. This trend is produced by the marker and formation energy methods. They are also shallower for the AB configuration. The shallow position of the levels might explain why they were undetected in DLTS studies,[21,22] though they are consistent with the IR-absorption experiments.[20]

We have also looked for a stable, doubly positive charge state for X-H complexes. However, as reported in Table VI, their second ionization energies are larger than the band gap, and therefore these defects are single donors only.

A Mulliken bond population analysis (Table VI) revealed the character of the donor state. The localization and s, p components of the wave function (η^2, α^2, and β^2, respectively) at the H and X atoms can be compared with ENDOR measurements by Zevenbergen *et al.*[18] and Huy *et al.*[19] Both NL54 and NL55 possess spin densities of $\sim 6\%$ and $\sim 0.3\%$ on sulfur and H atom, respectively. These are in good agreement with our calculations for both configurations. However, the larger s-orbital component of the wave function on the sulfur atom in NL54 suggests an assignment to S-H_{BC}, while NL55 could be assigned to S-H_{AB}.

These assignments are supported by inspection of the spin densities on the proton. For the S-H_{BC} defect, the p character of the wave function is much larger than the s character in line with observations on NL54.[19] Hence, the calculations support an assignment of NL54 and NL55 to two nearly degenerate S-H complexes, with BC and AB structures, respectively.

Now we turn to Se-H defects. Two Se-H related EPR signals are also known, and labeled NL60 and NL61. Both of these have properties in common with Se-H_{AB}. The spin densities on ^{77}Se are about 6% and 3%, with nearly equal s and p characters while the anisotropic components of the ^{1}H-related hyperfine tensors are similar to each other. NL60 can be distinguished form NL61 by the larger spin localization on the proton on the former ($\sim 0.5\%$), when compared with the latter defects (about 0.06% for each H atom). These properties are consistent with an assignment of both NL60 and NL61 to S-H_{AB} and suggest that one of the defects may be perturbed by a remote impurity.

We have also calculated the local vibrational mode frequencies for all stable complexes. These are shown at the bottom of Table VI. Clearly, we can distinguish the AB structures, which produce singlet-stretch and doublet-bend modes at around 1800 and 800 cm^{-1}, respectively, from the BC structures with modes at around 2100 and 600 cm^{-1}. Note that their spectral location is close to that of known antibonding Si-H and bonding Si-H oscillators.[42,43] Calculations by Liang *et al.*[26] have predicted a value of 1545 cm^{-1} for the Si-H stretching frequency in Te-H_{AB}. However, for Sb-H defects in a 32-Si-atom supercell, they reported frequencies more than 150 cm^{-1} below observations. Similar conditions led also to an underestimate in the frequency for the P-H defect, but the error turned to be considerably smaller (20 cm^{-1}) when using 64-atom cells.[44] No vibrational mode frequencies of S-H and Se-H complexes have, to our knowledge, been reported so far.

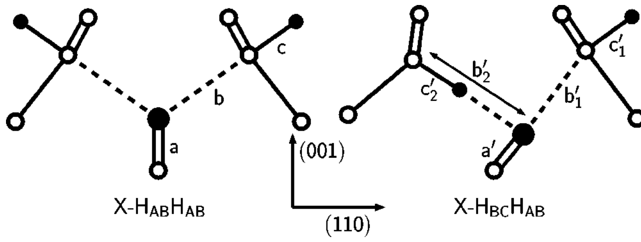

FIG. 6. Low-energy structures for X-H_2 complexes in silicon. H atoms are referred as bond centered and antibonding with respect to its nearest Si atom (leading to structures X-$H_{AB}H_{AB}$ and X-$H_{BC}H_{AB}$). Si, X, and H atoms are shown as open, large-closed, and small-closed circles, respectively. Bond lengths and distances (labeled by a, b, c, a', b_i', and c_i') are reported in Table VII.

VI. INTERACTION WITH TWO HYDROGEN ATOMS

There are many possible places for attachment of a second H atom. We considered all combinations of antibonded (to Si and X atoms) and bond-centered H atoms, as well as H_2^*-like structures. The later defects have trigonal symmetry, where a X-Si unit is transformed into X-H$\cdots$Si-H, H-$X\cdots$H-Si, and H-$X\cdots$Si-H structures. Among all defects, only those shown in Fig. 6 have a particular low formation energy. All other structures are at least 1 eV less stable, and in some cases the X-H+H→X-H_2 reaction is endothermic. This includes the case where both H atoms are bond centered, which is the analog of the ground state of a VOH$_2$ complex, where V denotes a vacancy.[45] Structures $XH_{AB}H_{AB}$ and $XH_{BC}H_{AB}$ have C_{2v} and C_{1h} symmetry, respectively, and therefore the calculations do not support the assignment of NL61 to a Se-H_2 defect.

Substitutional chalcogen impurities with a nearby H_2 molecule were also investigated. The center of mass of the molecule was placed at T_{Si} and T_X sites (see Fig. 3). After relaxation the molecule was aligned along the [111] direction, but the resulting structures are metastable by more that 1 eV. In fact, the binding energy of H_2 to X_s was found to be negligible.

Structural details of $XH_{AB}H_{AB}$ and $XH_{BC}H_{AB}$ are reported in Table VII (see also Fig. 6). In both defects, two Si-X bonds are broken (dashed lines), and two Si-H bonds are created. This leads to two structures where all Si and X atoms are fourfold and two fold coordinated.

An important question here concerns the electrical activity of these defects. Figure 5 (lower insets) shows the one-electron band structures for the most stable X-H_2 complexes. Unlike X-H, they suggest that X-H_2 are all electrically inert. The calculated donor and acceptor levels all lie below and above the valence and conduction bands, respectively (Table VII). These results are also in line with the disappearance of all X_s-related DLTS levels in hydrogenated samples.[21]

Also in Table VII, we report on the binding energy of a neutral H atom to X-H. Comparing E_b from Tables VI and VII, we realize that a second proton is bound with a similar energy to the first. That means that the thermal stability of X-H_2 and X-H defects should be similar.

Table VII gives the calculated LVM's for the X-H_2 defects. Again, Si-H_{BC} and Si-H_{AB} stretch modes fall in the 2100 and 1800 cm^{-1} regions, respectively. These can be compared with the H_{AB}-related stretch mode frequencies of P-H, As-H, and Sb-H complexes, which lie at 1555, 1561, and 1562 cm^{-1}.[46] On the other hand, the Si-H_{AB} unit on the H_2^* defect is responsible for an absorption band at 1838 cm^{-1}.[42] Two additional pairs of Si-H bend modes ap-

TABLE VII. Calculated relative energies E_{rel} (eV), XH-H binding energies E_b (eV), donor and acceptor levels $E(0/+)$ and $E(-/0)$ (eV), and structural parameters (in angstrom, see also Fig. 6). Local vibrational mode frequencies ν (cm^{-1}) are labeled according to its representation within the respective point group and mode type (s for a Si-H stretch mode, and b for a Si-H bend mode).

X	S		Se		Te
Complex	AB,AB	BC,AB	AB,AB	BC,AB	AB,AB
E_{rel}	0.00	0.00	0.00	0.16	0.00
E_b	1.86	1.86	1.79	1.63	1.75
$E(0/+)-E_v$ MM(Si)	−0.05	−0.02	−0.01	−0.01	−0.02
$E_c-E(0/-)$ MM(Si)	−0.02	−0.06	−0.05	−0.08	−0.10
$E(0/+)-E_v$ FEM	−0.42	−0.38	−0.37	−0.36	−0.27
$E_c-E(0/-)$ FEM	−0.01	−0.05	−0.01	−0.04	−0.04
a, a'	2.232	2.225	2.354	2.332	2.533
b, b_1'	3.041	2.882	3.002	2.835	2.987
b_2'		3.560		3.608	
c, c_1'	1.554	1.565	1.559	1.546	1.561
c_2'		1.497		1.502	
ν^s	1837(A_1)	2160(A')	1809(A_1)	2138(A')	1796(A_1)
ν^s	1830(B_1)	1778(A')	1802(B_1)	1768(A')	1785(B_1)
ν^b	813(A_1)	769(A')	820(A_1)	765(A')	822(A_1)
ν^b	808(B_1)	750(A')	816(B_1)	747(A')	818(B_1)
ν^b	799(A_2)	580(A'')	809(A_2)	578(A'')	808(A_2)
ν^b	798(B_2)	562(A'')	808(B_2)	560(A'')	807(B_2)

pear above the Raman frequency. These are about 800 and 570 cm^{-1} when the complex possesses Si-H$_{BC}$ and Si-H$_{AB}$ units, respectively.

VII. CONCLUSIONS

We have investigated the structure and energetics of chalcogen and chalcogen-hydrogen complexes in Si using an *ab initio* method. The substitutional defects are favored over interstitial impurities by more than 3 eV. This contrasts strongly with oxygen. Pairing of chalcogen atoms (including mixed pairs) is favored by more than 1 eV, except for Te$_{2s}$ that shows a 0.5 eV binding energy. The calculated equilibrium concentration of substitutional sulfur exceeds values found experimentally, This discrepancy might be related to the difficulty of estimating the chemical potential, or that there is a substantial energy barrier at the surface preventing the incorporation of the impurity. It has to be noted that previous attempts to estimate impurity solubilities have been successful in the case of oxygen in Si,[28] but not for Sn in Si.[47]

The defects are double donors again in contrast with substitutional oxygen.[28] The electrical levels are investigated by two methods. We find that the formation energy method yields values far too deep while a method based on the calculation of ionization energies and electron affinities yields better results. The single- and double-donor levels of Se, Te, and chalcogen pairs are found to be within 0.08 eV of their observed values when comparison is made to the results for S. The spin density on the chalcogen and their pairs is also found to be in good agreement with EPR data.

The impurities strongly bind to one and two hydrogen atoms. For singly hydrogenated impurities, only the X-H$_{BC}$ and X-H$_{AB}$ structures have binding energies compatible with the thermal stability of the chalcogen-hydrogen defects. These binding energies increase with the size of the chalcogen impurity. From an analysis of the energetics and Mulliken bond populations, we assign NL54 and NL55 to S-H$_{BC}$ and S-H$_{AB}$, respectively, whereas NL60 and NL61 are assigned to Se-H$_{AB}$ complexes, one of which is perturbed by a remote atom. This is supported by results on X-H$_2$, where all stable complexes are electrically inert, diamagnetic, and without the observed trigonal symmetry. In the X-H$_2$ defects, both protons lie at antibonding sites with a nearest Si atom, except for an energetically competitive S-H$_{BC}$H$_{AB}$ structure. We understand this on the grounds of an impurity size effect, by noting that for oxygen, a O-H$_{BC}$H$_{BC}$ structure was previously found.[45]

All the X-H complexes are predicted to be shallow single donors with levels above those of the isolated substitutional chalcogen impurities. These results are consistent with observations of an effective-mass series of IR-absorption lines due to two S-H complexes with ionization energies observed at 135.07 and 135.45 meV. On the other hand, X-H$_2$ centers are all electrically inert. LVM frequencies are reported for all complexes, but we are not aware of any experimental data.

ACKNOWLEDGMENTS

We would like to thank the EPSRC in the United Kingdom and the FCT in Portugal for computational and financial support.

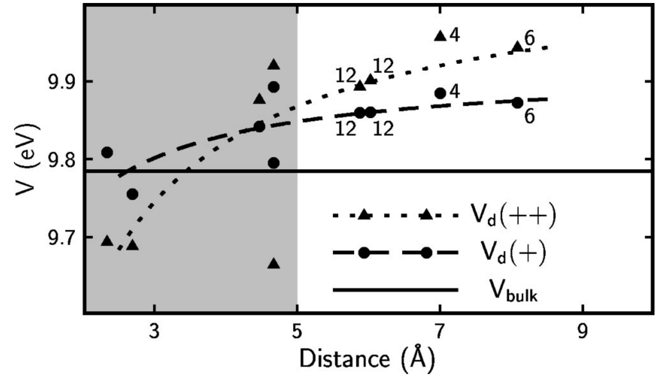

FIG. 7. Plot of the potential on T_d sites (eV) as a function of the distance (Å) from a substitutional sulfur impurity in the positive, $V_d(+)$, and double positive, $V_d(++)$, charge states. The potential in a bulk supercell ($V_{\rm bulk}$) is also shown as a horizontal line. Distant points are labeled according to the number of equivalent sites. All calculations used 64-Si-atom cells and the MP-2^3 scheme for **k**-point sampling. Curves are shown for guidance purposes only.

APPENDIX

As discussed in Sec. II, the valence-band top ($E_{\rm v}$) from Eq. (1) may be shifted from the bulk value $\epsilon^0_{\rm bulk}$ when a charged defect is introduced. This shift originates from the use of periodic boundary conditions where there is no reference for the average potential. We take the shift in the valence band to be given by the difference in potential (Hartree and local pseudopotential) between the defect and bulk at great distances from the defect.[9,48,49] This potential is, however, not easily evaluated. Here we estimate this shift $\bar{V}_{\rm bulk} - \bar{V}_{\rm d}$, by first calculating the difference in the potential, at all interstitial T-sites, in the bulk and defective cells. Then an average was taken over sites lying more than 5 Å away from sulfur (see Fig. 7). This average possesses a mean-square deviation of less than 0.03 eV.

In the FEM, the location of the $(q/q+1)$ energy level relative to the top of the valence band is given by the chemical potential $\mu_{\rm e}$ when $E_{\rm f}(q)=E_{\rm f}(q+1)$. Hence from Eq. (1),

$$E(q/q+1)-E_{\rm v}=E_{\rm d}(q/q+1)-\mathcal{E}_{\rm v}(q/q+1), \quad \text{(A1)}$$

with $E_{\rm d}(q/q+1)=E_{\rm d}(q)-E_{\rm d}(q+1)$, and $\mathcal{E}_{\rm v}$ is the crystal valence band top shifted by potential and monopole corrections; i.e.,

$$\mathcal{E}_{\rm v}(q/q+1)=\epsilon^0_{\rm bulk}-\bar{V}_{\rm bulk}+(q+1)\bar{V}_{\rm d}(q+1)-q\bar{V}_{\rm d}(q) + \frac{\alpha_{\rm M}}{L\epsilon}(2q+1). \quad \text{(A2)}$$

Values of these quantities are given in Tables III and II. It is noted that both the Madelung correction and potential corrections push the donor levels downwards.

In the MM(Si) method,[16] $\mathcal{E}_v(q/q+1)=E_{bulk}(q)-E_{bulk}(q+1)$. In this method, the monopole correction cancels, but the dispersion of either bulk- or defect-related bands can compromise the final result. This spurious effect is expected to be less in the MM(D) method, where the ionization energy of the defect is compared with that of a standard defect with similar donor/acceptor levels and wave functions of the same symmetry.[13]

*Electronic address: coutinho@fis.ua.pt

[1] H.G. Grimmeiss and E. Janzém, in *Deep Centers in Semiconductors*, 2nd ed., edited by S.T. Pantelides, (Gordon and Breach, Switzerland, 1996), p. 97.
[2] H. Overhof, M. Scheffler, and C.M. Weinert, Phys. Rev. B **43**, 12 494 (1991).
[3] G.W. Ludwig, Phys. Rev. **137**, A1520 (1965).
[4] E. Janzén, R. Stedman, G. Grossmann, and H.G. Grimmeiss, Phys. Rev. B **29**, 1907 (1984).
[5] H.G. Grimmeiss, E. Janzén, H. Ennen, O. Schirmer, J. Schneider, R. Wörner, C. Holm, E. Sirtl, and P. Wagner, Phys. Rev. B **24**, 4571 (1981).
[6] P. Wagner, C. Holm, E. Sirtl, R. Oeder, and W. Zulehner, in *Festkörperprobleme, Advances in Solid State Physics*, edited by P. Grosse (Vieweg, Braunschweig, 1984), Vol. 25, p. 191.
[7] S.D. Brotherton, M.J. King, and G.J. Parker, J. Appl. Phys. **52**, 4649 (1981).
[8] Y. Bar-Yam and J.D. Joannopoulos, Phys. Rev. B **30**, 1844 (1984).
[9] A. García and J.E. Northrup, Phys. Rev. Lett. **74**, 1131 (1995).
[10] M. Pesola, J. von Boehm, T. Mattila, and R.M. Nieminen, Phys. Rev. B **60**, 11 449 (1999).
[11] G.K. Wertheim, Phys. Rev. **105**, 1730 (1957).
[12] G.D. Watkins and J.W. Corbett, Phys. Rev. **121**, 1001 (1961).
[13] A. Resende, R. Jones, S. Öberg, and P.R. Briddon, Phys. Rev. Lett. **82**, 2111 (1999).
[14] J. Coutinho, R. Jones, P.R. Briddon, S. Öberg, L.I. Murin, V.P. Markevich, and J.L. Lindström, Phys. Rev. B **65**, 014109 (2002).
[15] T.A.G. Eberlein, C.J. Fall, R. Jones, P.R. Briddon, and S. Öberg, Phys. Rev. B **65**, 184108 (2002).
[16] Ji-Wook Jeong and A. Oshiyama, Phys. Rev. B **64**, 235204 (2001).
[17] S.J. Pearton, J.W. Corbett, and M. Stavola, *Hydrogen in Crystalline Semiconductors* (Springer-Verlag, Berlin 1992).
[18] I.S. Zevenbergen, T. Gregorkiewicz, and C.A.J. Ammerlaan, Phys. Rev. B **51**, 16 746 (1995).
[19] P.T. Huy, C.A.J. Ammerlaan, T. Gregorkiewicz, and D.T. Don, Phys. Rev. B **61**, 7448 (2000).
[20] R.E. Peale, K. Muro, and A.J. Sievers, Mater. Sci. Forum **65-66**, 151 (1990).
[21] G. Pensl, G. Roos, C. Holm, E. Sirtl, and N.M. Johnson, Appl. Phys. Lett. **51**, 451 (1987).
[22] G. Roos, G. Pensl, N.M. Johnson, and C. Holm, J. Appl. Phys. **67**, 1897 (1990).
[23] Z.N. Liang and L. Niesen, Phys. Rev. B **51**, 11 120 (1995).
[24] A.S. Yapsir, P. Deák, R.K. Singh, L.C. Snyder, J.W. Corbett, and T.-M. Lu, Phys. Rev. B **38**, 9936 (1988).
[25] V.J.B. Torres, S. Öberg, and R. Jones, in *Proceedings of the Shallow-Level Centers in Semiconductors'7, Amsterdam, 1996*, edited by C.A.J. Ammerlan and B. Pajot (World Scientific, Singapore, 1997), p. 501.
[26] Z.N. Liang, P.J.H. Denteneer, and L. Niesen, Phys. Rev. B **52**, 8864 (1995).
[27] R. Jones and P.R. Briddon, in *Identification of Defects in Semiconductors*, edited by M. Stavola Semiconductors and Semimetals, Vol. 51A (Academic Press, New York, 1998), p. 287.
[28] J. Coutinho, R. Jones, P.R. Briddon, and S. Öberg, Phys. Rev. B **62**, 10 824 (2000).
[29] J.P. Perdew and Y. Wang, Phys. Rev. B **45**, 13 244 (1992).
[30] G.B. Bachelet, D.R. Hamann, and M. Schlüter, Phys. Rev. B **26**, 4199 (1982).
[31] H.J. Monkhorst and J.D. Pack, Phys. Rev. B **13**, 5188 (1976).
[32] M.J.P. Musgrave and J.A. Pople, Proc. R. Soc. London, Ser. A **268**, 474 (1962).
[33] J.E. Northrup and S.B. Zhang, Phys. Rev. B **47**, 6791 (1993).
[34] G. Makov and M.C. Payne, Phys. Rev. B **51**, 4014 (1995).
[35] E.A. Walters and N.C. Blais, J. Chem. Phys. **80**, 3501 (1984).
[36] H. Pettersson and H.G. Grimmeiss, Phys. Rev. B **42**, 1381 (1990).
[37] *CRC Handbook of Chemistry and Physics*, 81st ed. edited by D. R. Lide (CRC, Boca Raton, 2000).
[38] A.B. van Oosten and C.A.J. Ammerlaan, Phys. Rev. B **38**, 13 291 (1988).
[39] J.R. Niklas and J-M. Spaeth, Solid State Commun. **46**, 121 (1983).
[40] S. Greulich-Weber, J.R. Niklas, and J-M. Spaeth, J. Phys.: Condens. Matter **1**, 35 (1989).
[41] C.G. Van de Walle, Phys. Rev. Lett. **64**, 669 (1990).
[42] J.D. Holbech, B. Bech Nielsen, R. Jones, P. Sitch, and S. Öberg, Phys. Rev. Lett. **71**, 875 (1993).
[43] E.V. Lavrov, J. Weber, L. Huang, and B.B. Nielsen, Phys. Rev. B **64**, 035204 (2001).
[44] Y. Zhou, R. Luchsinger, and P.F. Meier, Phys. Rev. B **51**, 4166 (1995).
[45] V.P. Markevich, L.I. Murin, M. Suezawa, J.L. Lindström, J. Coutinho, R. Jones, P.R. Briddon, and S. Öberg, Phys. Rev. B **61**, 12 964 (2000).
[46] K. Bergman, M. Stavola, S.J. Pearton, and J. Lopata, Phys. Rev. B **37**, 2770 (1988).
[47] M. Kaukonen, R. Jones, S. Öberg, and P.R. Briddon, Phys. Rev. B **64**, 245213 (2001).
[48] C.G. Van de Walle and R.M. Martin, Phys. Rev. B **35**, 8154 (1987).
[49] S. Pöykkö, M.J. Puska, and R.M. Nieminen, Phys. Rev. B **53**, 3813 (1996).